ISSN 0001-4338, Izvestiya, Atmospheric and Oceanic Physics, 2022, Vol. 58, No. 2, pp. 168–177. © Pleiades Publishing, Ltd., 2022.
Russian Text © The Author(s), 2022, published in Izvestiya Rossiiskoi Akademii Nauk, Fizika Atmosfery i Okeana, 2022, Vol. 58, No. 2, pp. 194–204.

About the Annual Course of Moscow Heat Island and the Impact on It of the Quarantine Measures to Prevent the COVID-19 Pandemic in 2020

M. A. Lokoshchenko[a], * and L. I. Alekseeva[a]

[a] *Lomonosov Moscow State University, Moscow, 119991 Russia*

**e-mail: loko@geogr.msu.su*

Received June 21, 2021; revised October 26, 2021; accepted December 8, 2021

Abstract—Seasonal differences in the Moscow urban heat-island intensity (UHII) have been studied in detail based on data obtained in 2018–2020 by the meteorological network of stations located in Moscow and Moscow region. It is shown that the annual cycle of this phenomenon is slightly pronounced. In most cases, the UHI is manifested stronger in summer and weaker in winter; however, in some months, the situation may be reverse. The question of the statistical significance of seasonal differences remains open. The closest statistical relationship was revealed between the UHI and lower clouds during the night hours, so that its highest intensity is observed in the least cloudy seasons (usually in summer). The UHII distribution functions are close to the normal law in summer and spring, and, in winter and fall, they are characterized by a noticeable positive asymmetry, because their values decrease and the mode approaches the lower physical limit. The period of strict quarantine restrictions during the COVID-19 pandemic in the spring and early summer of 2020 led to a rapid and statistically significant decrease in the Moscow UHII, probably due to both natural factors (increased cloudiness) and human activities (rapidly decreased anthropogenic heat fluxes and a weakened urban industrial haze creating an additional counterradiation).

Keywords: urban heat-island intensity, air temperature, seasonal differences, statistical significance, cloudiness, COVID-19 pandemic, anthropogenic heat flux

DOI: 10.1134/S0001433822020086

1. INTRODUCTION

The task of the authors is to analyze seasonal differences in the Moscow urban heat-island intensity (UHII) and how it was affected by the quarantine measures (the lockdown period) during the first wave of the COVID-19 pandemic in 2020. It is known that heat islands are created due to differences in the radiation balance (urban–rural differences in surface albedo, intensifying counterradiation by an industrial haze), a decrease in the consumption of heat required for the evaporation of precipitations (due to their artificial runoff) and for the transpiration from plants (the number of which is less within the city), direct heat emissions resulting from human activities; and other factors [1, 2]. The reasons for the occurrence of this phenomenon may also include a high heat capacity of asphalt and concrete in cities (walls of buildings, road surfaces, etc.). However, this factor leads not to the formation of heat islands, but rather to a time shift in the diurnal cycle of their intensity: their intensification early at night due to cooling inertia and their attenuation (or even the formation of short-lived "cool islands") in cities early in the morning due to the inertia of heating up these surfaces. It is also known that heat islands are highly dependent on synoptic conditions: they intensify within anticyclones under calm and clear weather conditions.

The question of annual UHII variations in the middle latitudes is nonobvious. In winter, when urban heating systems operate, the anthropogenic heat emissions are more significant. On the other hand, in summer, there are fewer losses through precipitation evaporation and transpiration in plants in the heat balance of cities when compared to rural areas. Moreover, in summer, the zonal transport becomes weaker in middle latitudes and air stagnations with clear and still nights intensifying heat islands are more often observed. However, heat islands may also intensify in winter under clear anticyclonic weather conditions during severe frosts. Thus, different factors variously affect the annual cycle of heat islands. For Moscow, with averaging over different periods, quite opposite conclusions about the annual UHII cycle were obtained: e.g., the UHII maximum was noted in winter [3] and summer [4]. It was shown in [5] that the seasonal features of the Moscow UHII are ambiguous. A separate study was needed to clarify this question and the effect of a rapid decrease in human activities during the lockdown period on the UHII.

It is very difficult to estimate the anthropogenic heat flux in cities, because direct measurement of it is impossible. However, evidently, its highest values are observed within the heating season in the middle and high latitudes. Sometimes, this flux is either neglected, if summer conditions are considered [6], or it is considered a remainder term in calculating the heat balance. However, in this case, its estimates include (comparable with its values) errors in determining other terms, which, sometimes, leads to unreal conclusions of its negative values in summer [7]. In most studies, the anthropogenic heat flux is indirectly estimated based either on generalized data for large areas, or on its estimates obtained for individual small objects and their expansion to a scale of the whole city [2]. The anthropogenic heat-flux estimates given in [8] according to the number of buildings and cars releasing heat and the rate of metabolism of the total number of residents may serve as an example of the first approach, and the estimates given in [9] for the power consumption of each individual building and their generalization per unit area using large-scale maps may serve as an example of the other approach. The calculation results differ enormously from place to place: from 12–13 W/m^2 in the Vancouver suburbs (Canada) [8] to 1590 W/m^2 in the center of Tokyo (Japan) [9]; according to generalized data, from 5 to 160 W/m^2, on average, per year for any city [2]. According to the estimates given in [10], the anthropogenic heat flux contributes to the heat-island formation over Tomsk (Russia) of 40–50% (~20–25 W/m^2) in summer and 80–90% (~70–75 W/m^2) under Siberian severe winter conditions. In addition to the direct effect of heat emissions, heat islands also form due to anthropogenic changes in the radiation balance and other heat balance fluxes. The 2020 global quarantine associated with the COVID-19 pandemic opened up a unique possibility to estimate the intensity of urban heat islands under the conditions of a rapid decrease in both direct and indirect anthropogenic factors when compared to normal conditions in other years.

2. SEASONAL FEATURES OF THE MOSCOW HEAT ISLAND

We have used air-temperature data obtained in 2018–2020 at conventional manned weather stations located in Moscow (all five stations) and the Moscow region (13 of 14 stations). The Nemchniovka station is excluded from the analysis due to its border location (in the vicinity of the Moscow Ring Road, which is the traditional city boundary), because this station consistently gives values that are intermediate between the urban and rural stations [11]. We used two indicators of the UHII—ΔT_{MAX} and ΔT_{av} (maximum and average (over the city area) intensities) [12]:

$$\Delta T_{MAX} = T_C - \frac{\sum_{j=1}^{m} T_{R_j}}{m}; \quad (1)$$

$$\Delta T_{av} = \frac{T_C + \sum_{i=1}^{n} T_{U_i}}{n+1} - \frac{\sum_{j=1}^{m} T_{R_j}}{m}, \quad (2)$$

where T_C is the air temperature at the station in the center of the city, T_U is the air temperature at the other urban stations, T_R is the air temperature at the rural stations, n is the number of stations located on the outskirts of the city, and m is the number of stations located in the rural zone in the vicinity of the city (in our case, $n = 4$ and $m = 13$). The maximum intensity is more indicative of differences between the city and its surroundings if a chosen station is located within the most densely built-up zone (which, in general, may be located not necessarily in the center of the city, but in any part of it). However, it is sensitive to the quality of data obtained at the only station chosen for comparison with background conditions. Moscow is convenient for studying urban climatology due to its simple geometric form that is close to an ellipse (within the conventional boundaries until 2012) and a general decrease in the housing density from the center of the city to its boundaries. Since 1946, Balchug has been the central station, located 600 m from the center of Moscow Kremlin, the data of which better reflect the influence of the city when compared to other stations. Unlike ΔT_{MAX}, average intensity ΔT_{av} takes into account data obtained at all stations within the city and, therefore, is more reliable; however, it more weakly reflects the influence of the city.

Figures 1a–1c give the calculations results for ΔT_{MAX} and ΔT_{av} for the Moscow conditions for every day over 3 years. It is seen that there are no unambiguous seasonal differences: they are masked by a high interdiurnal variability. Table 1 gives the average values and standard deviations of both parameters. It is seen that, within the annual cycle, the highest UHII is observed in summer or, in rare cases, in spring (ΔT_{av} for 2019). The lowest UHII is usually observed in winter; however, the ΔT_{av} values for the falls of 2018 and 2020 and the spring of 2020 during the quarantine restrictions proved as low as in winter. It is evident that, in Moscow, the UHII rapidly decreased in all seasons of 2020 and, on average, for 2020 when compared to the two previous years.

On average, over the 3 years (the size of both samples is 1096 daily means), the highest and average intensities of the Moscow heat island amounted to 2.0 and 1.0°C, respectively, as before, on average, for the 2010–2014 period [12]. Note a close relationship between both characteristics: the coefficient of their correlation for the entire 3-year sample is $R = 0.90$. A slight scatter in the values is associated with various

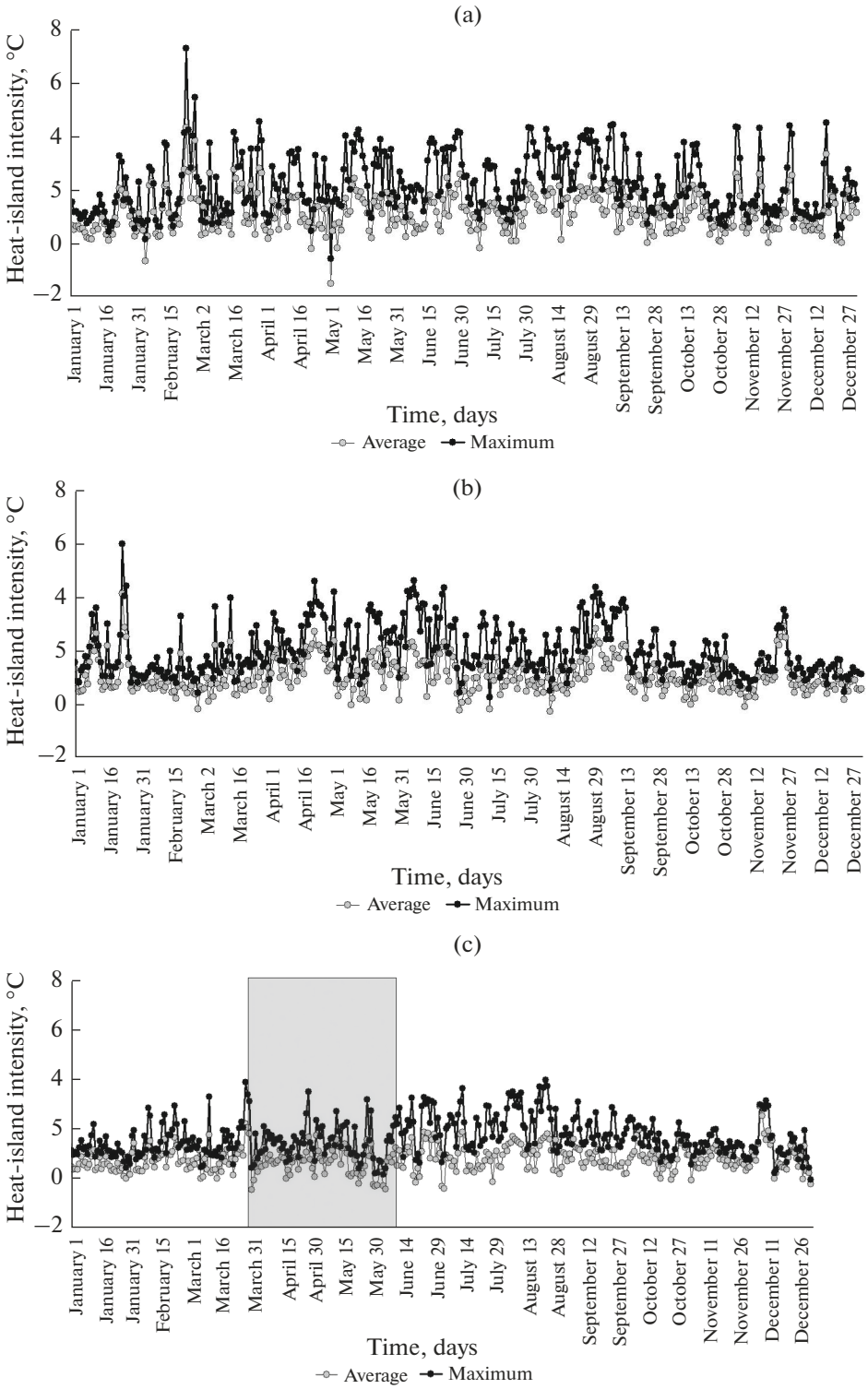

Fig. 1. Annual variations in the Moscow heat-island intensity in 2018–2020: (a) daily means of ΔT_{MAX} and ΔT_{av} for 2018, (b) daily means of ΔT_{MAX} and ΔT_{av} for 2019, (c) daily means of ΔT_{MAX} and ΔT_{av} for 2020, and (d) daytime and nighttime values of ΔT_{MAX} for 2018. The lockdown period due to the COVID-19 pandemic in 2020 is marked in gray.

degrees of the thermal inhomogeneity of the capital (differences between data obtained at the Balchug station and the other four urban stations) on some days. Over the 3 years, the record-high values of ΔT_{MAX} and ΔT_{av}, on average, per day amounted to 7.4 and 4.4°C, respectively, and were noted on February 23, 2018, when Moscow was within a low-gradient baric field in the vicinity of the ridge axis in the anticyclone system

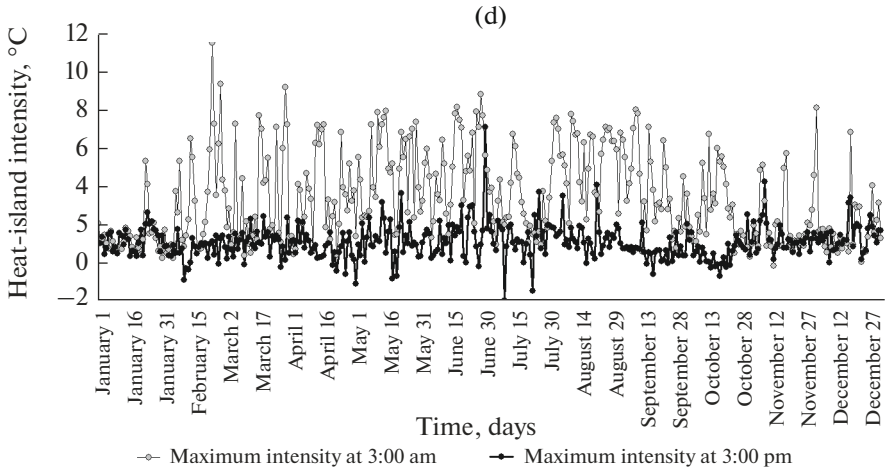

Fig. 1. (Contd.)

with its center over Belorussia. The pronounced anticyclonic conditions manifested themselves in a clear sky and calm at night: ΔT_{MAX} individually calculated for 3:00 am amounted to 11.5°C (Fig. 1d).

Conversely, the heat island effect is extremely slight or even vanishes under conditions of strong winds in zones of gradient currents at the periphery of deep cyclones and continuous cloudiness and heavy precipitation in frontal zones. In 2018–2020, the smallest values of ΔT_{MAX} and ΔT_{av} amounted to –0.6 and –1.5°C, respectively, in the warm-front zone on May 1, 2018. It is very rare that the values of both parameters are close to zero or even slightly negative: over the 3 years, ΔT_{av} was <0 only 26 times (in 2% of cases); moreover, it was never less than –0.6°C, except for May 1, 2018, and ΔT_{MAX} was negative only once.

Let us estimate the validity of differences between the seasonal averages of both UHII parameters. For such estimates, the Student criterion Z is usually used:

$$Z = \frac{(\bar{X} - \bar{Y})}{\sqrt{\sigma^2(X)/n + \sigma^2(Y)/m}}, \quad (3)$$

where X and Y are the mathematical expectations of both samples, $\sigma^2(X)$ and $\sigma^2(Y)$ are their variances, and n and m are their size. However, this criterion is parametrical and, strictly speaking, applicable only if both sampling distributions correspond to the normal law. Our case is not exactly the same. Only the intensity distributions for the summer and spring months are comparatively close to the normal distribution. Thus, in the example given in Fig. 2a for the summer of 2018, the value of χ^2 (the Pearson criterion) amounts to 6.02 with seven degrees of freedom for ΔT_{av} and 5.48 with four degrees of freedom for ΔT_{MAX}. Accordingly, the probability of errors in rejecting the null hypothesis for the correspondence of the sampling distribution to the normal law in both cases is high: 0.54 and 0.24 for the average and maximum intensities, respectively. However, in winter, the distributions of both characteristics do not correspond to the normal law because of their positive asymmetry resulting from their general decrease and the mode approaching to the lower physical limit (the coefficient of asymmetry A is close to zero for summer distributions, from 0 to 1 for spring distribu-

Table 1. Moscow heat-island intensity in different seasons and, on average, per year

	Winter	Spring	Summer	Fall	Year
Maximum intensity ΔT_{MAX}					
2018	1.8 ± 1.2	2.3 ± 1.1	2.7 ± 1.0	2.1 ± 1.0	2.2 ± 1.1
2019	1.5 ± 0.8	2.2 ± 0.9	2.3 ± 1.0	1.8 ± 0.9	1.9 ± 1.0
2020	1.4 ± 0.7	1.6 ± 0.7	2.2 ± 0.9	1.6 ± 0.5	1.7 ± 0.8
Average intensity ΔT_{av}					
2018	1.1 ± 0.9	1.2 ± 0.7	1.3 ± 0.6	1.1 ± 0.6	1.2 ± 0.7
2019	0.9 ± 0.6	1.2 ± 0.6	1.1 ± 0.6	1.0 ± 0.6	1.0 ± 0.6
2020	0.8 ± 0.5	0.8 ± 0.5	0.9 ± 0.6	0.8 ± 0.4	0.8 ± 0.5

The former values correspond to means, and the latter ones correspond to rms deviation.

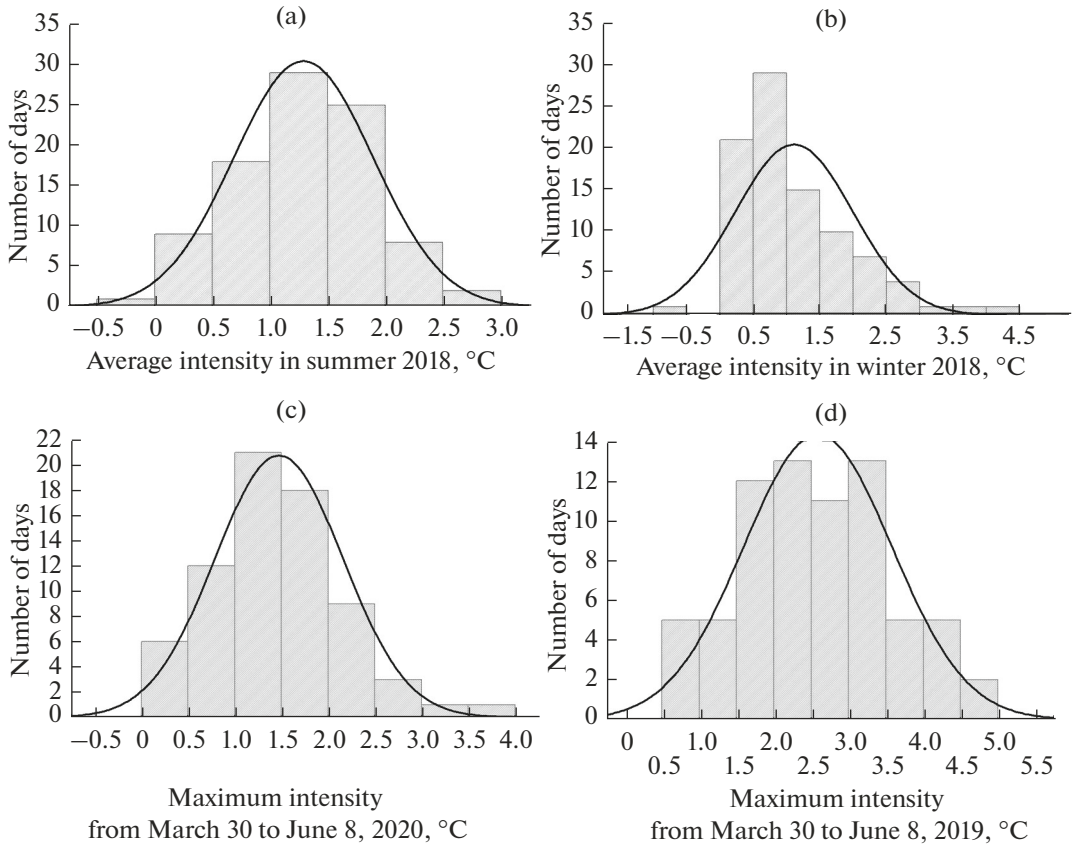

Fig. 2. Distribution of the Moscow heat-island-intensity values for individual periods and seasons: (a) ΔT_{av} for the summer of 2018, (b) ΔT_{av} for the winter of 2018, (c) ΔT_{MAX} for the quarantine period in 2020, and (d) ΔT_{MAX} for the same period in 2019.

tions, about 1 for fall distributions, and from 1 to 3 for winter distributions). Thus, in Figs. 2a and 2b, A is 0.03 and 1.87 for the summer and winter of 2018, respectively.

If the distribution functions slightly differ from the normal law, the Student criterion may approximately be used for qualitative estimates; however, the boundaries of confidence probabilities may be shifted. Table 2 gives the results of calculations (3) for the paired comparisons of different seasons. The Z values (in bold type) given in Table 2 correspond to statistically significant differences with a confidence probability of 0.99 provided that the sampling distributions are close to the normal law.

It is seen that the winter UHII differs most sharply from the summer UHII. The slightest differences in the UHII are observed in comparing its fall and winter characteristics and its fall and spring characteristics. In the latter case, the sole exception is the abnormally anticyclonic spring of 2019 that resulted in even a slightly higher value of ΔT_{av} for this season when compared to summer. Note also that the differences in the maximum intensity are more pronounced than those in the average intensity (in 17 of 18 cases), only except for the comparison between the spring and fall of 2020.

Since, in our case, using the Student criterion yields only qualitative comparative reliability estimates, we will also consider the nonparametric Wilcoxon test that is free from the initial hypothesis of the type of distribution. This test is based on the ranking of random variables in both samples and the summation of shifts in the values in both directions; and, in fact, it reduces to calculating the number of inversions

Table 2. Student criterion Z values in estimating seasonal differences in the Moscow heat-island intensity

	Winter–Summer	Winter–Spring	Winter–Fall	Summer–Spring	Summer–Fall	Spring–Fall
2018	**–5.4** (–1.6)	**–2.9** (–0.8)	–2.1 (–0.3)	2.6 (0.8)	**3.6** (1.5)	0.9 (0.6)
2019	**–5.9** (–2.3)	**–5.6 (–3.2)**	–2.6 (–1.5)	0.6 (–0.8)	**3.4** (0.8)	**3.0** (1.7)
2020	**–6.7** (–1.4)	–1.3 (0.8)	–2.2 (–0.2)	**5.3** (2.1)	**5.4** (1.4)	–0.6 (–1.1)

The former values correspond to maximum intensity, and the latter ones in round brackets correspond to average intensity.

(reverse shifts compared to ordinary differences) in testing the null hypothesis of the random character of differences. Calculations based on daily means of ΔT_{MAX} showed that, when the 3 winter and the 3 summer months are compared with each other using year 2018 as an example, the number of inversions (excesses of winter values over summer ones) is 1992 at sample sizes of 90 and 92. This is a significantly smaller value than $(m \times n/2) = 4140$ that characterizes the number of equally probable shifts in both directions. However, the Wilcoxon criterion is usually used for small samples with size $n = 25$ or, less commonly, $n = 50$. The results of recalculations for comparisons of partial samples composed of the first 25 days of the months of 2018—December–June, January–July, February–August, and December–August—showed the numbers of inversions: 127, 153, 152, and 72, respectively, at $(m \times n/2) = 312.5$. The Wilcoxon critical values at $n = 25$ amount to 100 and 76 for significance levels of 5 and 1%, respectively. It is seen that, in three of the four cases, the empirical values exceed theoretical ones even with a relatively soft significance level of 5%, which supports the null hypothesis of insignificant differences. The differences are reliable with confidence probability $P = 0.99$ only in comparing August and December. For this sample, the number of inversions was calculated based also on the ΔT_{av} data and amounted to 132, so that the differences between daily means of the average intensity according to the Wilcoxon criterion are insignificant even at $P = 0.95$ (132 > 100). It is evident that, in the other cases, the differences between the ΔT_{av} values are even more insignificant.

Additional calculations were performed based on nine average decade (10-day-period) values of ΔT_{MAX} for the winter and summer months of all 3 years. The inversion numbers amounted to 10, 9, and 9 for 2018, 2019, and 2020, respectively, at critical values of 8 and 3 with significance levels of 5 and 1%. Consequently, in all three examples, the differences are insignificant even at $P = 0.95$. It should be noted that the average value of ΔT_{MAX} for the third decade of February 2018 (4.2°C) significantly exceeded all 27 average 10-day-period values for the summer months of the 3 years. Thus, the question of the significance of the differences in ΔT_{MAX} and ΔT_{av} between the winter and summer months, strictly speaking, remains open (the validity of these differences according to Student criterion Z is unreliable due to asymmetric distribution functions in winter).

3. RELATIONS BETWEEN THE URBAN HEAT-ISLAND INTENSITY AND CLOUDINESS

To clarify the reasons for such seasonal differences, the ΔT_{MAX} and ΔT_{av} values were calculated individually for midnight and midday using the year 2018 as an example (the ΔT_{MAX} variations at 3:00 am and 3:00 pm for all days of this year are given in Fig. 1d). It is known that heat islands are more pronounced in darkness; in fact, the annual averages of ΔT_{MAX} and ΔT_{av} amount to 3.4 and 1.9°C for 3:00 am and only 1.1 and 0.4°C for 3:00 pm, respectively. In addition, it follows from Fig. 1d that, during the year, their daytime values vary slightly within a narrow range—as a rule, from 0 to 2°C (the limiting values are −2.0°C for July 9 and 7.1°C for June 30). The rms deviations σ for a whole sample of 365 values for 3:00 pm amount to only 0.9°C for ΔT_{MAX} and 0.7°C for ΔT_{av}. The night values are more variable: at 3:00 am, σ reaches 2.3 and 1.4°C for ΔT_{MAX} and ΔT_{av}, respectively, and the limiting values of ΔT_{MAX} amount to −0.2°C for November 11 and 11.5°C for February 23. It is seen that the night values of ΔT_{MAX} exhibit rapid nonperiodic variations; moreover, the heat island may be strongly pronounced ($\Delta T_{MAX} > 5$°C) up to seven to eight nights in a row. Such synoptic periods with a stably strong heat island are more often observed within both warm and transition seasons but may also be observed in winter (Fig. 1d, the third 10-day period of February). Their relationship with anticyclonic conditions—primarily, a small amount of clouds—is obvious.

Based on the 2018 data, both UHII indicators were compared with different meteorological parameters (total and low cloudiness, average and maximum wind velocities, daily air-temperature amplitudes, and others) according to data obtained at Moscow State University's Meteorological Observatory (MSU MO). This comparison showed that the UHII indicators are most closely related to cloudiness. In fact, the coefficients of correlation R of ΔT_{MAX} and ΔT_{av} with total cloudiness amounted to −0.58 and −0.50 and, with low cloudiness, amounted to −0.67 and −0.61, respectively, for 3:00 am. It is not surprising that heat islands are more closely related to low clouds if a comparatively weak effect of sparse upper-level clouds (Ci and others) on the surface radiation balance is considered. For 3:00 pm, all values of R are insignificant (<0.1), which is also not surprising because the portion of counterradiation in the total daytime radiation balance is insignificant.

To estimate possible nonlinear relations, the values of η^2 (the index of confidence of their description by the sixth degree power function) were used, because, for the function of such a high order, η may be considered a rough estimate of the correlation ratio. It turned out that, in all four cases, $(\eta^2 - R^2) < 0.1$ for the midnight, so that the nonlinear component of the relations is insignificant, and the R values may be used in analyzing these relations [13]. Their significance is beyond question. Thus, according to the Student criterion, using the sampling validity threshold, we have

$$t = \frac{R}{\sigma_R},$$

where $\sigma_R = \frac{\sqrt{1-R^2}}{\sqrt{n-2}}$ is the error of the correlation coefficient at a large size of sample n, the values of t for all the four coefficients of correlation of nighttime data amount to 11–17 in absolute value. Since the threshold value of t at 363 degrees of freedom and a significance level of 0.001 amounts to 3.3, all four relations of both total and lower clouds with ΔT_{MAX} and with ΔT_{av} at 3:00 am are statistically significant with P that is much higher than 0.999. Note that the t criterion is parametric; however, at large ($n > 100$) samples and R values that are far from 0 and 1, its application is possible even without a special estimation of the type of distribution [13].

Nevertheless, for a higher validity of the conclusion, we will also use the Fisher nonparametric Z-test to estimate the significance of R:

$$t_z = \frac{Z}{\sigma_z},$$

where $Z \approx \frac{1}{2}\ln\frac{1+R}{1-R}$, $\sigma_z = \frac{1}{\sqrt{n-3}}$. The values of t_z are also extremely high in absolute magnitude (from 10 to 15). Thus, the statistical significance of the relations of the UHII with the total and low cloudiness during the night hours at $P \gg 0.999$ is supported by both criteria.

This result makes it possible to conclude that the relations between the UHII and night cloudiness are much more pronounced than its differences between the calendar seasons. In other words, the Moscow UHII is more strongly pronounced within a season with a smaller amount of clouds during the night hours; this usually occurs in summer, because the summer nights are, as a rule, less cloudy. However, in cold winters with dominating anticyclonic weather conditions and clear nights, the UHII is more strongly pronounced than in summer under cloudy weather conditions. Thus, in the very cold and mainly anticyclonic February 2018, the Moscow UHII, on average per month, was more strongly pronounced ($\Delta T_{MAX} = 2.3°C$, $T_{av} = 1.5°C$) than in the cloudy July 2018 with dominating cyclonic weather conditions ($\Delta T_{MAX} = 2.0°C$, $\Delta T_{av} = 1.0°C$). The monthly average low cloudiness in February, which was anomalously low for winter (6.4 for the daily average and 6.0 for 3:00 am), proved almost equal to the anomalously high (for summer) lower cloudiness in July (6.2 for the daily average and 5.8 for 3:00 am). Apparently, in February, the heat island was additionally intensified by heat emissions from urban heating systems. Thus, the differences in the estimates of the annual heat-island cycle in the past were most likely associated with long-term variations in dominating synoptic conditions and, as a consequence, nighttime cloudiness in different seasons.

4. THE MOSCOW HEAT ISLAND DURING THE QUARANTINE OF 2020

Let us consider variations in the Moscow UHII within the period of quarantine measures (the lockdown period) at the height of the first wave of the COVID-19 pandemic in 2020. Closing or slowing down the operation of industrial enterprises under quarantine conditions and a rapid decrease in the traffic intensity may result not only in reduced anthropogenic heat emissions, but also in radiation-balance changes—first and foremost, in a vanished or attenuated urban industrial haze generating counterradiation. At the same time, the available satellite data on heat islands within the surface-temperature field during the global quarantine of spring 2020 are ambiguous. In some places, their attenuation was noted: on average, by 20% for the eight largest cities in Pakistan [14] and for cities in the United Arab Emirates [15]. In April 2020, even a rather cold island in the surface temperature field was observed over the urban zone of New Delhi [16]. By contrast, according to satellite data obtained in the spring of 2020, in cities within the Indus and Ganges river basins, the surface heat islands intensified by 0.2–0.4°C during daylight hours, because a quarantine-induced delay in harvesting winter crops led to an additional vegetation of rural areas and, as a consequence, an increase in heat consumption for plant transpiration [17].

In Moscow and other Russian cities, the most severe quarantine restrictions were implemented only from the spring to early summer of 2020 within the first wave of the pandemic (later, in the fall, with the arrival of the second wave of the pandemic, the reintroduced lockdown regime was incomplete). In Moscow, the lockdown was introduced partially on March 28 and finally on March 30, being finally cancelled starting on June 9. Thus, the possible differences in the start date of this period amount to 2 days. Let us consider this period within the boundaries of lockdown for the entire metropolitan population except for emergency workers—71 days from March 30 to June 8. According to data given in [18], during this lockdown, the surface content of basic pollutants in the atmosphere over Moscow decreased, on average, by 30–50%, and the traffic intensity reduced even more—it was four times lower in April 2020 than in April 2019.

There are two approaches in estimating the validity of differences in the UHII: to compare the lockdown period with the same time periods in other years or with the time before and after the lockdown period in 2020. The latter approach is also quite suitable, because the lockdown period mainly concurred with the transitional spring season, so that basic differences in the annual cycle between the summer and winter should not manifest themselves in comparison results.

It follows from Table 3 that, on average, within the lockdown period from March 30 to June 8, 2020, both intensity parameters were anomalously low

Table 3. Moscow heat-island intensity during the quarantine period in 2020 in comparison with other periods, °C

Qua	Quarantine 30/3–8/6, 2020	Ibid, 30/3–8/6, 2019	Ibid, 30/3–8/6, 2018	Period 1–29/3 and 9/6–31/12, 2020
ΔT_{MAX}	1.5 ± 0.7	2.6 ± 1.0	2.3 ± 1.0	1.7 ± 0.8
$\Delta T_{av.}$	0.7 ± 0.5	1.3 ± 0.6	1.1 ± 0.7	0.9 ± 0.5

The former values correspond to means, and the latter ones correspond to rms deviations.

($\Delta T_{MAX} = 1.46$°C, $\Delta T_{av} = 0.66$°C). At the same time, in previous years, the average values of ΔT_{MAX} and ΔT_{av} were significantly higher: 2.31 and 1.12°C for 2018 and 2.57 and 1.34°C for 2019, respectively. The distribution function of these parameters, especially ΔT_{MAX}, are, on the whole, close to the normal law: thus, the values of the Pearson criterion χ^2 for the ΔT_{MAX} distribution amount to only 2.92 for the lockdown period of 2020 and 2.43 for the same time period in 2019 (Figs. 2c, 2d). This implies a very high probability of errors in rejecting the null hypothesis of compliance with the normal law—0.82 and 0.66 for 2020 and 2019, respectively. Thus, in contrast to the analysis of seasonal differences, here, using Student parametric criterion Z is completely appropriate. Its values in estimating differences between the lockdown period of 2020 and the same time periods in the previous years proved extremely high: 5.84 and 4.54 for comparison with 2018 and 7.79 and 6.95 for comparison with 2019 for ΔT_{MAX} and ΔT_{av}, respectively. Thus, according to the Student criterion, the differences between the sampling mathematical expectations are reliable with a confidence probability of much higher than 0.999 (i.e., with a significance level of much less than 0.001).

For an additional validation of the significance of the differences according to the Wilcoxon criterion, seven average values of ΔT_{MAX} were calculated for individual 10-day periods, including the first 10-day period (which increased by 2 days, March 30 and 31) of April and the first incomplete (8-day) 10-day period of June. It turned out that, for a number of these 10-day-period averages for 2020, there is not a single inversion in comparing them with similar data series either for 2019 or 2018. In other words, the highest value of seven averages of ΔT_{MAX} for 2020 is smaller than its lowest value of seven averages for both 2019 and 2018. According to the Wilcoxon criterion, this implies the significance of the differences with the same high confidence probability (0.999) as is the case with the use of the Student criterion.

The value of Z was 3.04 and 2.92 for ΔT_{MAX} and ΔT_{av}, respectively, in comparing average heat-island intensities during the quarantine period and the remaining 295 days of 2020, which also supports the validity of the differences with a confidence probability of 0.99.

Thus, both approaches to the comparison showed that, during the period of strict quarantine restrictions, such a decrease in the heat-island intensity was evident and statistically significant. This decrease includes both natural and anthropogenic components. The former component is associated with clouds that attenuate the UHII (stable feedbacks of the heat-island intensity with cloudiness, especially nighttime clouds, were already noted above). May and early June 2020 were anomalously cloudy. May 2020 with an average total and lower cloudiness of 7.9 and 6.3 (at a climatic normal of 6.8 and 4.3), respectively, ranked seventh in the list of the cloudiest months of May since 1954 according to data obtained at the MSU MO. It should be noted that May and June 2020 were the rainiest these months (170 mm and 193 mm, respectively) throughout the 200-year period of precipitation measurements in Moscow.

Figure 3 (in addition to Fig. 1c) shows the mean-diurnal ΔT_{MAX} variations for the time span between March 12 and June 30, 2020, including the quarantine period. Figure 3 also shows variations in the total daily amount of lower clouds according to MSU MO data and in the traffic intensity according to data obtained at the Moscow Transport Department and collected by A.S. Ginzburg (until the end of May) [18]. It is seen that a stable inverse dependence of the UHII on cloudiness was also observed within this period; this dependence especially manifests itself in an anomalously weak heat island under the conditions of continuous dense clouds, for example, from May 30 to June 4, when Moscow was within the zones of atmospheric fronts at the near periphery of the cyclone with its center over Ukraine.

In addition to cloudiness, let us also consider two more meteorological parameters based on MSU MO data—daily average wind velocity V according to M-63 instrument data obtained at a height of 15 m and the amplitude of daily variations in T. Increased wind velocity, as well as cloudiness, leads to a decrease in the intensity of heat islands but to a lesser degree. The air-temperature amplitude (the difference between maximum and minimum values of T for every day) does not directly affect heat islands but serves as a good indicator of anticyclonic weather conditions under which heat islands are more pronounced. Table 4 gives the correlation-analysis results. It is seen that the relations of both UHII characteristics with the meteorological

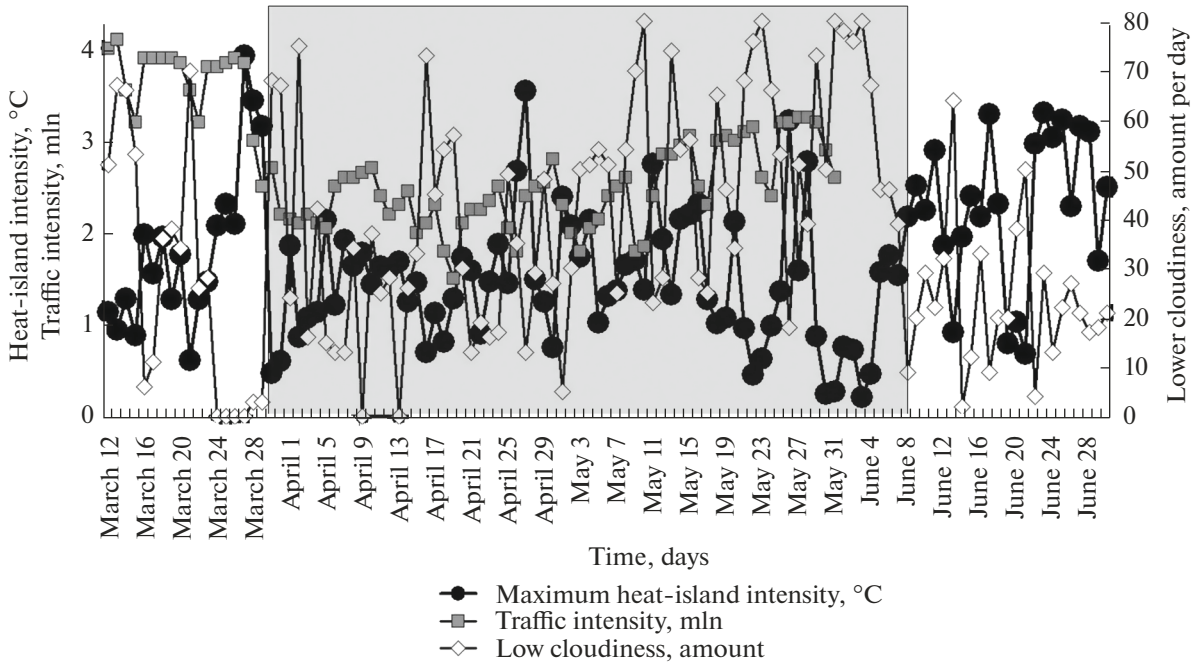

Fig. 3. Variations in the Moscow heat-island intensity and the factors presumably affecting it in March–June 2020. The lockdown period due to the COVID-19 pandemic in 2020 is marked in gray.

parameters are statistically significant, but they are only moderate, not close. The coefficient of multiple correlation of the maximum UHII with lower cloudiness and V, which reflects the combined effect of both meteorological parameters on ΔT_{MAX}, amounts to –0.78.

Thus, cloudiness itself, considered separately from the anthropogenic factors and even with consideration for the wind-velocity effect, cannot provide a complete explanation for the anomalously weak UHII during the quarantine in Moscow. In fact, while May 2020 was unusually cloudy in Moscow, April 2020, on the contrary, was characterized by a smaller average amount of total and low cloudiness (7.0 and 3.8, respectively) when compared to the climatic normal. At the same time, the average UHII for these two months turned out anomalously low and almost the same: 1.51 and 0.74°C in April and 1.56 and 0.72°C in May for ΔT_{MAX} and ΔT_{av}, respectively. The Moscow UHII was anomalously low (see Table 3), on average, for the entire quarantine period, although the degree of cloud cover, on average, for April and May (7.45/5.05 for total/lower cloudiness) only slightly exceeded their general climatic normals (by 0.3 and 0.4 for the total and lower cloudiness, respectively). On the other hand, in other much cloudier months of recent years, the Moscow UHII was much more pronounced. Thus, in the very cloudy July 2018 and July 2019 with an average cloud amount of 8.2/6.2 and 8.2/5.9, the values of ΔT_{MAX} and ΔT_{av} amounted to 2.0 and 0.9°C, respectively, in both cases.

Therefore, in addition to increased cloudiness, there is a noticeable anthropogenic component that is responsible for the attenuation of the Moscow UHII during the quarantine period. It is likely that this atten-

Table 4. Coefficients of correlation R of natural and anthropogenic indicators with the Moscow heat-island intensity for a period of March 12 to June 30, 2020

	Average intensity ΔT_{av}, °C	Maximum intensity ΔT_{MAX}, °C
Total cloudiness, daily amount	–0.40	–0.40
Low cloudiness, daily amount	–0.64	–0.67
Daily average wind velocity for 15 m V, m/s	–0.28	–0.43
Daily air-temperature amplitude, °C	0.43	0.56
Traffic intensity, personal vehicles, mln transported people [18]*	0.06	0.09

* Estimates of R for the period March 12–May 31, 2020.

uation was mainly caused by decreased direct anthropogenic-heat emissions and a decreased industrial haze generating counterradiation due to the shutdown of many industrial enterprises. Unfortunately, total estimates of industrial emissions on certain days of the Moscow quarantine, if they exist, are unknown to us. As for the data given in Fig. 3 on the traffic intensity of the Moscow road network, they are statistically unrelated to the UHII (Table 4). This indicator apparently either does not reflect real variations in the radiation balance of the urban atmosphere or its estimates according to data obtained by the Moscow Transport Department within the quarantine period are insufficiently accurate.

5. CONCLUSIONS

(1) The annual cycle of the Moscow UHII is rather weakly pronounced. The UHII is usually maximum in summer and minimum in winter; however, in some cases, the situation may be the opposite.

(2) Of natural (nonanthropogenic) factors, the UHII is most closely related to low cloudiness at night; it is most pronounced in months and seasons with clear nights or nights with a small amount of clouds (as a rule, in summer).

(3) The lockdown period during the COVID-19 pandemic from March to June 2020 was characterized by a rapid and statistically significant attenuation of the Moscow UHII due to both natural factors (increased cloudiness) and human activities (decreased anthropogenic heat emissions and a decreased industrial haze due to a rapid reduction of industrial emissions and traffic intensity).

ACKNOWLEDGMENTS

We thank N.A. Tereshonok and N.S. Nikolaev from the Central Administration of the Russian Hydrometeorological Service for providing observational data obtained at meteorological stations located in Moscow and Moscow region.

CONFLICT OF INTEREST

The authors declare that they have no conflict of interest.

REFERENCES

1. H. E. Landsberg, *The Urban Climate* (Academic Press, New York, 1981).
2. T. R. Oke, G. Mills, A. Christen, and J. A. Voogt, *Urban Climates* (University Press, Cambridge, 2017).
3. M. A. Lokoshchenko and A. A. Isaev, Influence of Moscow city on the air temperature in Central Russia, in *Proc. 5th International Conference on Urban Climate (ICUC)*, Lodz, Poland, 2003, Vol. 2, pp. 449–453.
4. K. G. Rubinshtein and A. S. Ginzburg, "Estimation of air temperature and precipitation changes in large cities (by example of Moscow and New York)," Russ. Meteorol. Hydrol. **28** (2), 20–26 (2003).
5. *The Climate of Moscow in Global Warming Conditions*, Ed. by A. V. Kislov (MGU, Moscow, 2017) [in Russian].
6. C. S. B. Grimmond and T. R. Oke, "Comparison of heat fluxes from summertime observations in the suburbs of four North American cities," J. Appl. Meteorol. **34** (4), 837–889 (1995).
7. B. Offerle, C. S. B. Grimmond, and K. Fortuniak, "Heat storage and anthropogenic heat flux in relation to the energy balance of a Central European city centre," Int. J. Climatol. **25**, 1405–1419 (2005).
8. C. S. B. Grimmond, "The suburban energy balance: Methodological considerations and results for a midlatitude west coast city under winter and spring conditions," Int. J. Climatol. **12** (5), 481–497 (1992).
9. T. Ichinose, K. Shimodozono, and K. Hanaki, "Impact of anthropogenic heat on urban climate in Tokyo," Atmos. Environ. **33** (24), 3897–3909 (1999).
10. N. D. Dudorova and B. D. Belan, "Assessment of factors controlling the formation of urban heat island in the city of Tomsk," Opt. Atmos. Okeana **29** (5), 426–436 (2016) [in Russian].
11. L. I. Alekseeva, "Features of the Moscow urban heat island in 2018 in the surface layer according to meteorological network data," in *Environmental and Climate Characteristics of the Atmosphere in Moscow in 2018 According to the Measurements of the Moscow State University Meteorological Observatory*, Ed. by M. A. Lokoshchenko (MAKS Press, Moscow, 2019), pp. 95–110 [in Russian].
12. M. A. Lokoshchenko, "Urban heat island and urban dry island in Moscow and their centennial changes," J. Appl. Meteorol. Climatol. **56** (10), 2729–2745 (2017).
13. A. A. Isaev, *Statistics in Meteorology and Climatology* (Izd. MSU, Moscow, 1988) [in Russian].
14. G. Ali, S. Abbas, F. M. Qamer, et al., "Environmental impacts of shifts in energy, emissions, and urban heat island during the COVID-19 lockdown across Pakistan," J. Cleaner Prod. **291**, 125806 (2021).
15. A. S. Alqasemi, M. E. Hereher, G. Kaplan, et al., "Impact of COVID-19 lockdown upon the air quality and surface urban heat island intensity over the United Arab Emirates," Sci. Total Environ. **767**, 144330 (2021).
16. S. Mukherjee and A. Debnath, "Correlation between land surface temperature and urban heat island with COVID-19 in New Delhi, India," Res. Square (2020). https://doi.org/10.21203/rs.3.rs-30416/v1.
17. T. C. Chakraborty, S. Chandan, and X. Lee, "Reduction in human activity can enhance the urban heat island: Insights from the COVID-19 lockdown," Environ. Res. Lett. **16**, 054060 (2021).
18. A. S. Ginzburg, V. A. Semenov, E. G. Semutnikova, et al., "Impact of COVID-19 lockdown on air quality in Moscow," Dokl. Earth Sci. **495** (1), 862–866 (2020).

Translated by B. Dribinskaya